DOI: 10.1002/ejic.200700078

NMR Studies of Paramagnetic Metallocarbaporphyrinoids

Ewa Pacholska-Dudziak[a] and Lechosław Latos-Grażyński*[a]

Keywords: Carbaporphyrinoids / Porphyrinoids / NMR spectroscopy / Organometallic chemistry

Carbaporphyrinoids provide a suitable macrocyclic platform for organometallic investigations that provide unique opportunities for modifying a macrocyclic structure. Alteration of a coordination core is a route of choice for stabilizing unusual metal ion oxidation states and coordination geometries. This microreview presents the general characteristic of paramagnetic metallocarbaporphyrinoids, with a focus on NMR studies. NMR spectroscopy of paramagnetic molecules can be considered as a powerful probe of several intriguing aspects of the molecular and electronic structures, structural rearrangements, and reactivity, including oxidation and oxygenation, of this fascinating class of compounds. The chosen examples address paramagnetic organometallic nickel(II) and nickel(III) complexes of *N*-confused porphyrins, the reactions of nickel(II) dimethylated *N*-confused porphyrins with organometallic reagents, the stabilization of rare organocopper(II) species, the investigation of weak intramolecular metal–arene interactions, and the conformational flexibility of nickel(II) benziporphyrin and vacataporphyrin. Particular emphasis is placed on NMR studies as an efficient way of detecting intermediate species formed in the course of oxidation and oxygenation of iron(*n*) carbaporphyrinoids.

Introduction

^{1}H NMR spectroscopy has been extensively applied to paramagnetic molecules including a variety of paramagnetic metalloproteins. The fundamental theoretical description of the electron–nucleus interaction, as reflected by the NMR parameters, illustrated by appropriate examples of applications has been presented in several monographic works.[1–10] In particular, the amount of NMR information provided by the contact shift and dipolar shift, and their temperature dependency, have been addressed. Relaxation phenomena related to the presence of unpaired electrons have also been a topic of some interest. Amongst others, the following subjects have been investigated: spin density delocalization correlated to the electronic structure, structural and electronic equilibria, the dynamics of intramolecular rearrangements, stereochemistry, solvation, and the structure of the second coordination sphere.

^{1}H NMR spectroscopy has been found to be a particularly useful method for detecting and characterizing iron complexes of porphyrins,[7] *N*-substituted porphyrins,[11–15] heteroporphyrins,[16–19] and hemoproteins in different coor-

[a] Department of Chemistry, University of Wrocław,
14 F. Joliot-Curie St., Wrocław 50 383, Poland

Ewa Dudziak (née Pacholska) was born in Wrocław, Poland, in 1969. She completed her PhD in 2000 under the supervision of Prof. Latos-Grażyński at the University of Wrocław, where she also obtained her BSc in 1993. She was a postdoctoral researcher in Dijon with Prof. Roger Guilard at the University of Burgundy, France. She is now working in Prof. Latos-Grażyński's group at the University of Wrocław on complexes of core-modified porphyrins with a flexible skeleton involved in organometallic coordination.

Professor Latos-Grażyński (the corresponding member of the Polish Academy of Sciences) is the Polish representative on the Editorial Board of this journal. Prof. Latos-Grażyński's involvement in porphyrin chemistry stems from his interest in the NMR of paramagnetic systems. Thus, much of his research has been devoted to the electronic structure and reactivity of paramagnetic metalloporphyrins, especially hemes. He has investigated model systems for heme enzymes, heme degradation, the activation of dioxygen by metalloporphyrins, the reactivity of metalloporphyrin π-radicals, and the properties of unusually oxidized systems, for example organocopper(II) species. The attention of Prof. Latos-Grażyński and his group is currently focused on the synthesis of novel porphyrinoids that have at least one of the regular pyrroles replaced by a carbo- or heterocyclic moiety. The organometallic species that can be made from carbaporphyrinoids are of special interest.

dination/oxidation states.[8,20] These studies have yielded an insight into the mechanisms of spin-density transfer in paramagnetic metalloporphyrins. In particular, it has been found that this technique is extremely sensitive toward fine structural effects such as substitution, electronic asymmetry, axial ligation (steric hindrance and basicity), or puckering of an equatorial macrocycle. Exchange and rotation of the molecular fragments have also been a subject of interest, and the intermediate iron porphyrin species that act in dioxygen activation or oxygen-atom transfer have been "trapped" by NMR spectroscopy.[21–23] Recently, octaethylporphyrin degradation (coupled oxidation) has been explored in order to establish the reactivity of iron complexes in various stages of heme degradation.[24–35] For instance, the paramagnetic shift patterns for the model iron octaethylbiliverdin-related radical complexes present several useful probes for detecting analogous species in hemoproteins by ^{1}H NMR spectroscopy.[35]

Recent progress in the ^{1}H NMR spectroscopic characterization of paramagnetic hemoproteins is related to the search for suitable spectroscopic models that involve the synthesis of fine-tuned iron porphyrins. These models mimic the spectroscopic properties encountered in hemoproteins for a given electronic state.[7] The application of two-dimensional techniques initially afforded an unambiguous assignment of resonances related to the active hemoprotein site and eventually yielded three-dimensional hemoprotein structures in solution.[8,20]

In light of the format of a microreview, here we intend to present an overview centered on our most recent efforts in the field of paramagnetic metallocarbaporphyrinoids, with a focus on the application of ^{1}H NMR spectroscopy to this unique class of compounds. Thus, variations of the porphyrin core involving the introduction of a hydrocarbon unit in place of one of pyrrolic nitrogens have led to a new class of macrocycles − carbaporphyrinoids (Scheme 1) − that have interesting properties both in terms of their aromatic character and their potential ability to bind metal ions.[36,37]

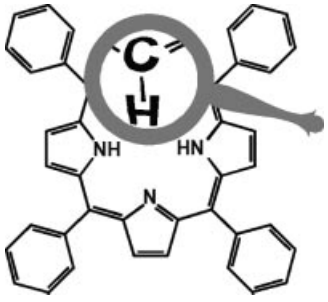

Scheme 1. A carbaporphyrinoid.

Such a replacement preserves three regular pyrrole moieties while the (C_nNNN) core determines the monocarbaporphyrinoid structure.[38–45] The internal carbon atom(s) belong(s) to the carbo- or heterocycles that replace(s) the original pyrrole ring of the porphyrin. In general, carbaporphyrinoids provide a unique molecular platform that is suitable for exploring organometallic chemistry in a peculiar macrocyclic environment and forcing an unusual coordination geometry and/or oxidation state of the metal ions.[39–41,44,45] Systematic, comprehensive summaries of the current state-of-the-art in carbaporphyrinoid chemistry are contained in several review articles.[38–46]

Carbaporphyrinoids

The synthesis of 2-aza-21-carba-5,10,15,20-tetraarylporphyrin ("inverted porphyrin", "*N*-confused porphyrin", "mutant porphyrin", "carbaporphyrin") was seminal for the field of cabaporphyrinoids.[36,37] An inverted porphyrin is a constitutional isomer of a porphyrin which preserves its general structural framework.[46,47] The synthesis of this molecule prompted intense synthetic work to generate a whole class of carbaporphyrinoids.[36–40,43–45,48–50]

Here, we have gathered together the representative structures of two tautomers of this *N*-confused porphyrin, namely (CP*H*)H$_2$ and (*H*CP*H*)H,[36,37] and the alkylated *N*-confused porphyrins (*R*CP*H*)H, (CP*R*)H$_2$ and (*R*CP*R*$_1$)-H,[44,51–55] *m*-benziporphyrin (*m*BP*H*)H,[56] *m*-benziporphodimethene (*m*BDM*H*)H,[57] *p*-benziporphyrin (*p*BP*H*$_2$)H,[57] vacataporphyrin (VP*H*$_2$)H,[58] and *N*-confused pyriporphyrin (*N*PyP*H*)H (3-aza-*m*-benziporphyrin)[59] that have been used in our laboratory to synthesize paramagnetic compounds for subsequent NMR investigation (Scheme 2).

We will use the symbol CP to denote the trianion obtained from the inverted porphyrin by abstraction of all pyrrolic NH protons and the *C*-bound H(21) hydrogen. The groups attached to the N(2) atom are indicated by a prefix in italics and the group attached to C(21) as a suffix in italics. A similar method is used to form acronyms for other carbaporphynoids, as shown above.

Paramagnetic Organometallic Nickel(II) *N*-Confused Porphyrin Derivatives

Methylation of a diamagnetic nickel(II) complex of [(*H*CP)Ni^{II}] with methyl iodide yields stable organonickel-(II) complexes (Scheme 3), namely diamagnetic [(CP*Me*)-Ni^{II}] and the two paramagnetic species [(*H*CP*Me*)Ni^{II}X] (X = Cl, I) and [(*Me*CP*Me*)Ni^{II}I].[52]

The mechanism of this methylation involves oxidative addition of the methyl cation to the carbaporphyrin C(21), which is activated due to Ni–C coordination. The concerted reversible addition of HX converts diamagnetic [(CP*Me*)-Ni^{II}] into paramagnetic [(*H*CP*Me*)Ni^{II}X]. The axial coordination step is accompanied by protonation of the peripheral nitrogen. The ^{1}H and ^{2}H NMR spectra of paramagnetic [(*H*CP*Me*)Ni^{II}X] and [(*Me*CP*Me*)Ni^{II}I] were analyzed by considering their C_1 symmetry (Figure 1). There are seven distinct pyrrole C-H positions for [(*H*CP*Me*)Ni^{II}X], an NH(2) position analogous to the CH(2) of the regular porphyrin, and four inequivalent *meso*-aryl rings. The resonances were assigned by making use of selective deuteration and 2D COSY experiments. Thus, the characteristic pattern of six downfield-shifted pyrrole resonances accompanied by

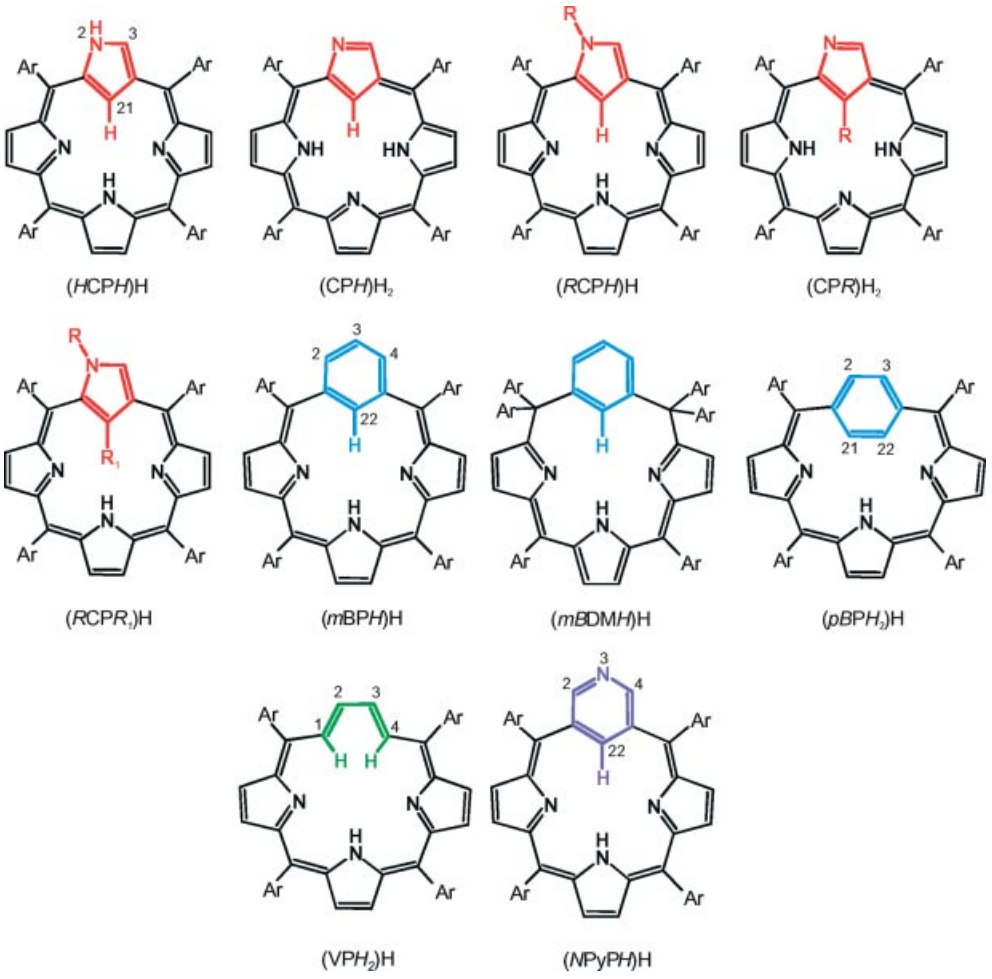

Scheme 2. Carbaporphyrinoids applied as ligands of paramagnetic complexes (partial numbering included).

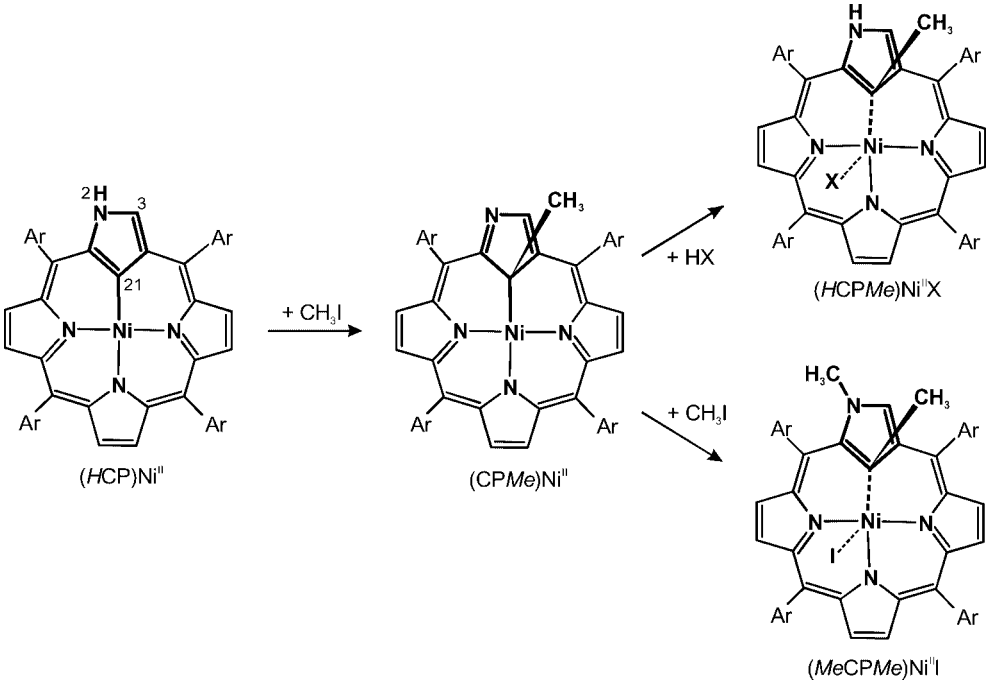

Scheme 3. Methylation of [(*H*CP)Ni^{II}] (X = Cl, I).

upfield-shifted H(3) and NH(2) resonances is diagnostic of *C*-methylation. The most characteristic feature, namely the broad downfield resonance (linewidth: 1320 Hz) at δ = 109.7 ppm, was assigned to the 21-Me group.

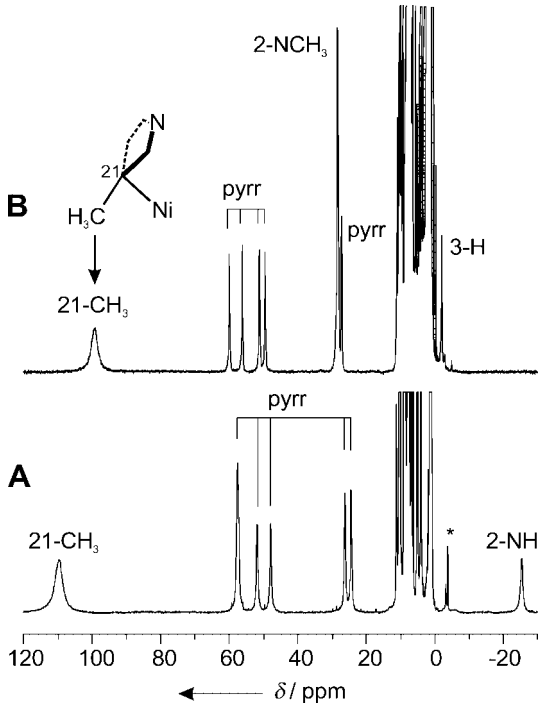

Figure 1. ^{1}H NMR spectra ($CDCl_3$, 293 K) of paramagnetic mono- and dimethylated nickel(II) carbaporphyrins [(*H*CP*Me*)Ni^{II}Cl] (A) and [(*Me*CP*Me*)Ni^{II}I] (B). The peak labels follow systematic numbering of the porphyrin ring or denote proton groups; pyrr: regular pyrrole ring protons. Reproduced, with permission, from ref.[52] Copyright 1996 American Chemical Society.

As in the case of methylation, the reaction of [(*H*CP)-Ni^{II}] with haloalkanes in the presence of proton scavengers yielded the C(21)-alkylated complexes [(CP*CH$_2$R*)Ni^{II}]. Protonation of the external nitrogen of the inverted pyrrole during HX addition (X = Cl, I) combines with coordination of the apical ligand and leads to paramagnetic nickel(II) complexes. A very strong differentiation of the isotropic shift for the diastereotopic methylene protons was observed in the ^{1}H NMR spectra of the protonated paramagnetic species [(*H*CP*CH$_2$*R)Ni^{II}X].[54]

The downfield shift of the pyrrolic and *C*-methyl resonances of [(*Me*CP*Me*)Ni^{II}X] indicates a σ-delocalization of the spin density. This is consistent with the ground state of Ni^{II}, which has two unpaired electrons in the σ-symmetry orbitals $(d_{x^2-y^2})^1(d_{z^2})^1$. The large differences in β-H contact shifts result from the π-spin density delocalized into the porphyrin framework, which originates from the peculiar spin-density transfer within the inverted pyrrole ring. The isotropic shift of the inverted *C*-methylated pyrrole ring is of significance with respect to the nature of the Ni–inverted pyrrole interaction in this paramagnetic organonickel(II) complex. The considerable downfield C(21)-CH_3 shift can be accounted for by direct σ-delocalization over three single bonds in the Ni–C(21)–$C_{(methyl)}$–H fragment. The tilt of the inverted *C*-methylated ring changes the geometry of the spin-density delocalization path as compared to regular pyrrole rings. The unpaired spin density is localized on the molecular orbital dominated by the p_z component, which can transfer the σ-spin density but simultaneously contributes to π-orbitals of the inverted pyrrole ring. Such an overlap within the inverted ring will permit direct transfer of the unpaired spin density of the C(21) p_z into the π system without any π M–L bonding.

Organometallic Ni^{III} Complexes

The one-electron oxidation of [(*H*CP)Ni^{II}] and [(*Me*CP)-Ni^{II}] results in the formation of extremely rare organonickel(III) derivatives.[60] The EPR spectral patterns of the one-electron-oxidized species depend on the axial ligand introduced by the oxidant or by metathesis. In each case the spin-Hamiltonian parameters [$g_{av} > 2.1$ (77 K) or $g_{iso} > 2.1$ (298 K)] reveal a metal-centered oxidation rather than formation of a radical cation ($g_{iso} \approx 2.002$). The localization of the one-electron oxidation on the nickel ion was supported by analysis of the observed ^{61}Ni hyperfine splitting. ^{2}H NMR spectroscopy was used as an independent probe to determine the electronic structure of the nickel(III). Such an approach can be complementary to the EPR studies and allows a direct observation of the spin-density delocalization on the macrocycle.

In light of the EPR results two representative species, namely [(D_7-*H*CP)Ni^{III}Br] and [(D_7-*H*CP)Ni^{III}(NO_3)] were selected for ^{2}H NMR investigation [(D_7-*H*CP)H has all β-positions substituted with deuterium]. The well-resolved EPR spectra of this complex suggest that its ^{1}H NMR resonances could be beyond detection due to the relatively long electron spin-lattice relaxation time T_{1e}.[9] Line widths for deuterium resonances are theoretically predicted to be 42 times smaller than the corresponding proton resonances due to the different electron-nuclear dipolar relaxation.[61] This narrowing has been observed experimentally for many paramagnetic species and renders ^{2}H NMR spectroscopy particularly useful in detecting those paramagnetically broadened resonances that are visible in the ^{1}H NMR spectrum.

In the case of [(D_7-*H*CP)Ni^{III}Br], all resonance peaks assigned to the pyrrole deuterons are located within the region δ = 2–8 ppm that is consistent with the $(d_{z^2})^1$ formulation of the electronic ground state (Figure 2, trace A). No spin density is present in the β-pyrrole positions since there is no overlap of the metal out-of-plane orbital with the ligand orbital. On the contrary, all but one pyrrole resonances of [(D_7-*H*CP)Ni^{III}(NO_3)] are shifted downfield and are widely spread, covering the δ = 0–50 ppm region (Figure 2, trace B). This downfield shift of the pyrrole resonances is indicative of σ-delocalization of the spin density and requires a considerable $d_{x^2-y^2}$ metal orbital contribution to the SOMO, as determined previously by EPR spectroscopy.

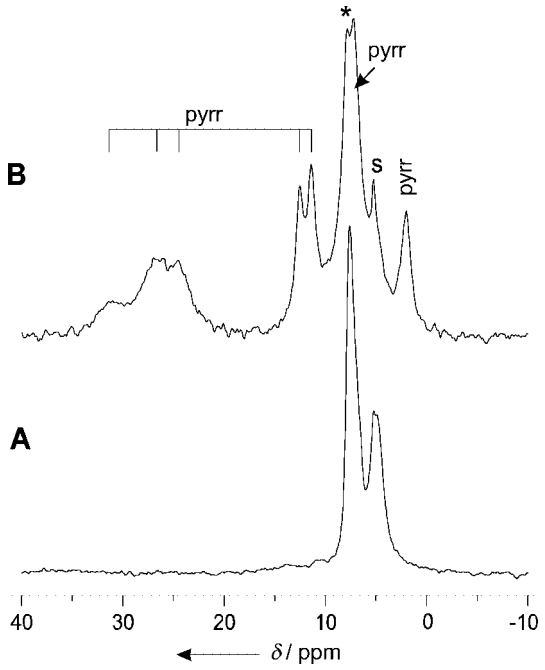

Figure 2. ^{2}H NMR spectra (298 K in CH_2Cl_2) of [(D_7-*H*CP)-Ni^{III}Br] (A) and [(D_7-*H*CP)$Ni^{III}(NO_3)$] (B); s: solvent. Reproduced, with permission, from ref.[60] Copyright 1997 American Chemical Society.

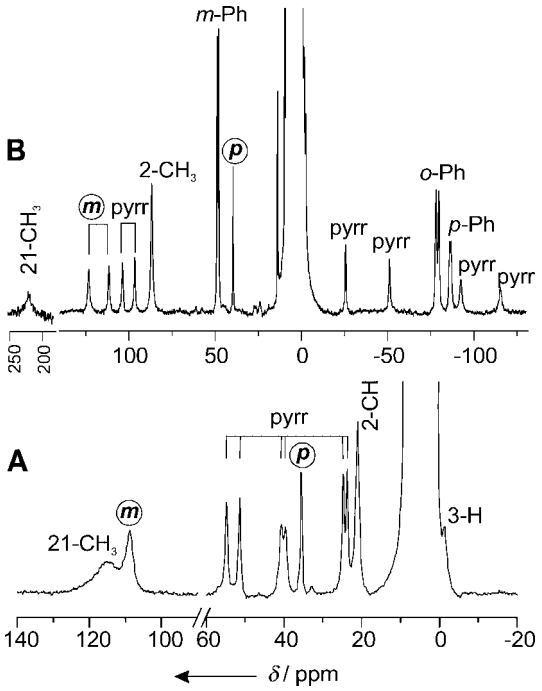

Figure 3. ^{1}H NMR spectra of [(*Me*CP*Me*)Ni^{II}Ph] (A; 293 K, C_7D_8) and [(*Me*CP*Me*)Ni^{II}Ph]$^-$ (B; C_7D_8, 253 K) formed by treating [(*Me*CP*Me*)Ni^{II}Cl] with phenyllithium in toluene at 203 K. The peaks of the Ni-coordinated phenyl group are marked by circles. Reproduced, with permission, from ref.[62] Copyright 2000 American Chemical Society.

Reactions of [(*Me*CP*Me*)Ni^{II}Cl] with Organometallic Reagents

Addition of phenylmagnesium iodide to a toluene solution of the nickel(II) chloride complex of dimethylated inverted porphyrin [(*Me*CP*Me*)Ni^{II}Cl] at 203 K results in the formation of a rare paramagnetic σ-phenylnickel(II) species [(*Me*CP*Me*)Ni^{II}Ph], which contains both equatorial and apical Ni^{II}–C bonds.[62] The coordination of the σ-phenyl group was determined by the unique pattern of three σ-phenyl resonances (*ortho*: δ = 361.3 ppm; *meta*: δ = 103.2 ppm; *para*: δ = 34.8 ppm at 273 K) in the ^{1}H and ^{2}H NMR spectra (Figure 3).

Predictably, the first step in the titration with phenyllithium results in the formation of [(*Me*CP*Me*)Ni^{II}Ph] and the subsequent one-electron reduction with excess PhLi yields [(*Me*CP*Me*)Ni^{II}Ph]$^-$, which can also be generated by an independent route, namely by reduction of [(*Me*CP*Me*)-Ni^{II}Ph] with lithium triethylborohydride or tetrabutylammonium borohydride. The spectroscopic data (Figure 3, trace B) indicate that [(*Me*CP*Me*)Ni^{II}Ph] undergoes a one-electron reduction without a substantial disruption of the molecular geometry. The presence of two paramagnetic centers in [(*Me*CP*Me*)Ni^{II}Ph]$^-$, namely the high-spin nickel(II) and the carbaporphyrin radical anion, produces a remarkable variation in the spectral pattern, such as upfield and downfield positions of the pyrrole resonances and a sign alternation of the *meso*-phenyl resonances.

A single species was detected in the ^{1}H NMR titration of [(*Me*CP*Me*)Ni^{II}Cl] with *n*-butyllithium. The formation of the one- or two-electron-reduced species {[(*Me*CP*Me*)-Ni^{II}Bu]$^-$ or [(*Me*CP*Me*)Ni^{II}Bu]$^{2-}$, respectively} can be considered to account for the peculiar spectroscopic properties [pyrrole: δ = 17.33, 15.45, –5.79, –7.74, –14.62, –58.14 ppm; CH_3(21): δ = 3 ppm at 203 K]. The temperature dependencies of the hyperfine shifts demonstrate the pronounced anti-Curie behavior, which was interpreted in terms of a temperature-dependent spin equilibrium.

Organocopper(II) *N*-Confused Porphyrin and Its Methylated Derivatives

The inverted porphyrin and its methylated derivatives stabilize the rare organocopper(II) complexes [(*H*CP)Cu^{II}], [(*Me*CP)Cu^{II}], [(*H*CP*H*)Cu^{II}X], [(*Me*CP*H*)Cu^{II}X] (X = Cl^-, $CF_3CO_2^-$), and [(*Me*CP*Me*)Cu^{II}Cl].[63] The EPR spectra of these complexes reveal typical features that are diagnostic of the copper(II) electronic structure.[63] In particular, the superhyperfine coupling pattern indicates the presence of three nitrogen donors in the first coordination sphere.[63,64] Addition of an acid (HX) to [(*H*CP)Cu^{II}] and [(*Me*CP)Cu^{II}] yields [(*H*CP*H*)Cu^{II}X] and [(*Me*CP*H*)Cu^{II}X], respectively. The mechanism of this reaction includes protonation of the inner C(21) accompanied by an axial coordination of the anion. The ^{2}H NMR investigations (Figure 4) carried out for the pyrrole deuterated derivatives [(D_7-CP)Cu^{II}] and [(D_7-*Me*CP*Me*)Cu^{II}Cl] and the methyl deuterated complex

[(CH_3CPCD_3)Cu^{II}Cl] independently confirmed the copper(II) electronic structure, which has a considerable $d_{x^2-y^2}$ metal orbital contribution to the SOMO.

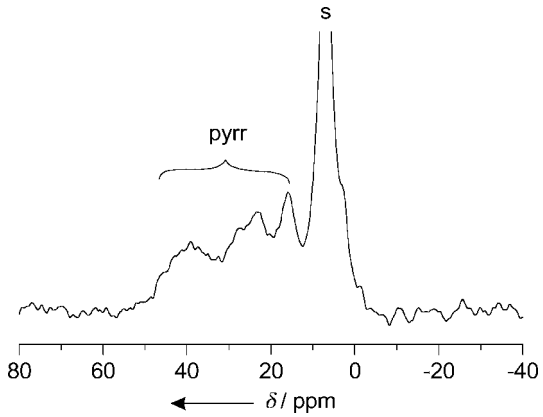

Figure 4. ^{2}H NMR spectrum of [(D_7-*H*CP)Cu^{II}] (333 K, toluene); s: solvent. Reproduced, with permission, from ref.[63] Copyright 2000 American Chemical Society.

Nickel(II) Complexes of Benziporphyrins – A Study of Weak Intramolecular Metal–Arene Interactions

Owing to the nonplanar coordination geometry of the metal ion the nickel complexes [(*m*BP*H*)Ni^{II}Cl] and [(*p*BPH_2)Ni^{II}Cl] are all paramagnetic, with $S = 1$.[65] The ^{1}H NMR spectra shown in Figure 5 correspond to effective C_s symmetry of the molecules. The observed pattern of chemical shifts is typical for high-spin Ni^{II} complexes of porphyrins and porphyrin analogues, with most of the β-H pyrrole resonances in the downfield region (δ = 10–60 ppm) and the *meso*-aryl peaks in the range δ = 0–10 ppm.[39] A similar spectroscopic pattern has been observed for [(*m*BP*OAc*)Ni^{II}Cl].[66] Almost complete assignment of these signals was achieved from the 2D COSY spectrum.

The shifts of the *m*-phenylene protons of [(*m*BP*H*)Ni^{II}Cl] are of special interest. The signals for H(2,4) and H(3) show evident sign alteration (δ = 22.5 and –40.8 ppm at 298 K, respectively). The broadened signal, which is shifted to δ = 386 ppm in the spectrum of [(*m*BP*H*)Ni^{II}Cl] (298 K), is assigned to the inner H(22). This is easily verified by acidifying a solution of ([*m*BP)Ni^{II}] with DCl rather than HCl. The resulting species, [(*m*BP*D*)Ni^{II}Cl], is selectively deuterated at position 22 and no low-field signal is observed. The above assignment also relied on the significant broadening of the H(22) signal relative to H(2,4), which is caused by the proximity of the paramagnetic Ni^{II} center. This argument was reinforced by a quantitative analysis of relaxation times, which yielded approximate distances between the nickel ion and certain protons in the molecule (Figure 6).[2,5,65] The ^{1}H NMR spectrum of [(*p*BPH_2)Ni^{II}Cl] appears to be similar to the preceding spectrum of [(*m*BP*H*)-Ni^{II}Cl] except that the *p*-phenylene resonances H(2,3) and H(21,22) are located at δ = –10.5 and 0.0 ppm, respectively (298 K), rather than in the far downfield region.

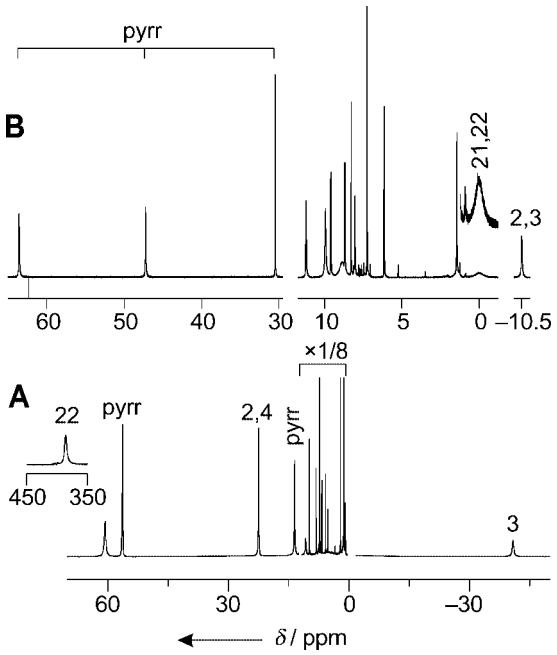

Figure 5. ^{1}H NMR spectra ($CDCl_3$, 298 K) of [(*m*BP*H*)Ni^{II}Cl] (A) and [(*p*BPH_2)Ni^{II}Cl] (B). Reproduced, with permission, from ref.[65] Copyright 2004 American Chemical Society.

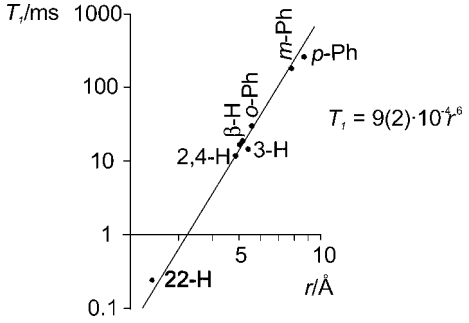

Figure 6. Relaxation plots for [(*m*BP*H*)Ni^{II}Cl]. The dependence between T_1 ($CDCl_3$, 298 K) and *r* (crystal structure averages) is linear in bilogarithmic axes.[65] Reproduced, with permission, from ref.[65] Copyright 2004 American Chemical Society.

X-ray studies performed on [(*m*BP*H*)Ni^{II}Cl] show that the arene fragment approaches the metal ion at a distance much shorter than the sum of the van der Waals radii, which corresponds to the formation of a weak agostic bond. Consequently, an agostic mechanism of spin-density transfer was proposed to explain the enormous H(22) shift as a result of electron donation from the CH bond to the metal. To account for the shifts of protons H(2,4) and H(3) it is necessary to assume π delocalization into the arene ring, which may result either from direct interaction with the metal center or from σ-π polarization.

Conformational Flexibility of Nickel(II) Benziporphyrins

The linewidths of certain signals for [(*m*BP*H*)Ni^{II}Cl] and [(*p*BPH_2)Ni^{II}Cl] exhibit an unusual temperature depen-

dence that is characteristic of a dynamic process.[67] This was interpreted in terms of an equilibrium wherein one of the forms is present at a very small concentration and cannot be observed directly. The two exchanging forms are only present at comparable concentrations, and therefore yield separate signals in the slow exchange limit, for the nickel(II) benziporphodimethene complex [(*m*BDM*H*)-Ni^{II}Cl]. A mechanism involving motion of the phenylene moiety was proposed to account for the observed exchange process (Scheme 4).

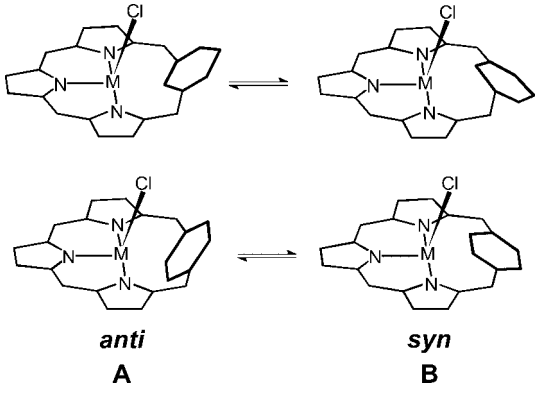

Scheme 4. Conformational equilibria in [(*m*BDM*H*)Ni^{II}Cl].

The temperature-dependence of the linewidths in the ^{1}H NMR spectrum of [(*m*BP*H*)Ni^{II}Cl] is shown in Figure 7 for the *m*-phenylene H(2,4) signal. The logarithm of $\nu_{1/2}$ is plotted against T^{-1} as this has often been found to yield a linear plot for a paramagnetic species in the absence of chemical exchange.[68,69]

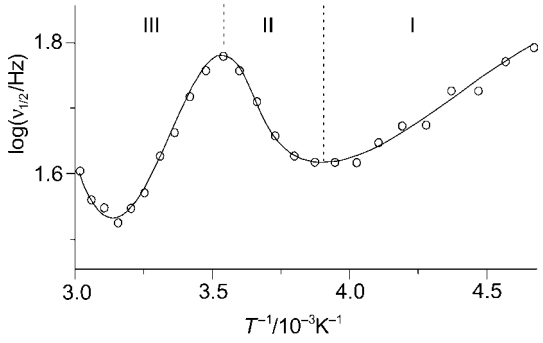

Figure 7. Temperature dependence of the linewidths in the ^{1}H NMR spectrum for H(2,4) of [(*m*BP*H*)Ni^{II}Cl] ($CDCl_3$, 213–333 K). The continuous line is for illustrative purposes only. Reproduced, with permission, from ref.[67] Copyright 2004 American Chemical Society.

The temperature profile (regions I–III) corresponds to an exchange process between two paramagnetic species A and B, one of which is significantly less populated ($P_A >> P_B$) and thus impossible to observe directly.[5,61,68] The dynamic process is slow in region I and the observed dependence may therefore be attributed solely to paramagnetic broadening and extrapolated into regions II and III.[68] The analysis concentrated on region II, which corresponds to the slow-exchange limit between A and B. The pre-exchange lifetime for A (τ_A) was obtained experimentally by determining line widths, $\nu_{1/2,A,i}$, over a wide temperature range, and an Eyring plot of the [(*m*BP*H*)Ni^{II}Cl] data for region II collected in deuterated chloroform yielded the activation parameters. The values $\Delta H^{\ddagger}$ = 63 kJ mol^{-1} and $\Delta S^{\ddagger}$ = 20 J/mol K yield a $\Delta G^{\ddagger}$ of 57 kJ mol^{-1} (298 K). These values are in the range found for various dynamic processes observed in porphyrins, including rotation of *meso*-aryl substituents and macrocycle inversion.[70–72]

Benziporphyrin macrocycles are generally more flexible than regular porphyrins, as can be judged from the puckered structures observed in the solid state for free bases and their complexes.[56,57,65,66] This is a result of the loss (or decrease) of macrocyclic aromaticity combined with the steric constraints generated by the introduction of a phenylene ring into the macrocyclic structure. Conformational dynamics involves puckering of the benziporphyrin macrocycle, rotation of *meso*-aryl rings, or both. The preferred conformation of the macrocycle in the metal complexes [(*m*BP*H*)-Ni^{II}Cl] and [(*p*BPH_2)Ni^{II}Cl] has the phenylene ring tilted away from the metal center with the inner CH bonds and the axial MX bond in an *anti* orientation (Scheme 4), as confirmed by their respective X-ray structures.[57,65] However, it is possible that minute amounts of *syn* conformers may be present in solution and rapidly equilibrate with the respective *anti* forms. Actually the DFT modeling, carried out for benziporphyrin complexes of zinc(II) and cadmium(II), indicates that the postulated *syn* conformers are thermally accessible.

Two Coordination Modes of Vacataporphyrin

5,10,15,20-Tetraaryl-21-vacataporphyrin (butadieneporphyrin, annulene-porphyrin hybrid),[58] which contains a vacant space instead of a heteroatomic bridge, forms paramagnetic nickel(II) complexes where a metal ion is bound in the macrocyclic cavity by three pyrrolic nitrogens.[73] Coordination imposes a steric constraint on the geometry of the ligand and leads to two directly detectable stereoisomers with the butadiene fragment oriented towards [(VPH_2)-Ni^{II}Cl-*i*] or away from [(VPH_2)Ni^{II}Cl-*o*] the macrocyclic center (Scheme 5).

The specific assignment of two sets of resonances to [(VPH_2)Ni^{II}Cl-*o*] and [(VPH_2)Ni^{II}Cl-*i*] (Figure 8) was based on the notion that the butadiene fragment in the folded conformation of [(VPH_2)Ni^{II}Cl-*i*] blocks the coordination of the second axial ligand, which contrasts with the behavior of [(VPH_2)Ni^{II}Cl-*o*].

The H(2,3) signals of [(VPH_2)Ni^{II}Cl-*o*] or [(VPH_2)-Ni^{II}Cl-*i*] have chemical shifts that are typical for the β-H pyrrolic positions of nickel(II) 21-heteroporphyrins in spite of the vacancy.[39] The extremely broad H(1,4) signal of [(VPH$_2$)Ni^{II}Cl-*o*] was detected by ^{2}H NMR spectroscopy at δ = –3.5 ppm (298 K).

A plot of $\log \nu_{1/2}$ against T^{-1} yields a straight line for [(VPH_2)Ni^{II}Cl-*i*], which suggests the absence of any chemical exchange.[18,19,39,52,67–69,74] On the other hand, the line widths of certain signals of [(VPH_2)Ni^{II}Cl-*o*] exhibit an un-

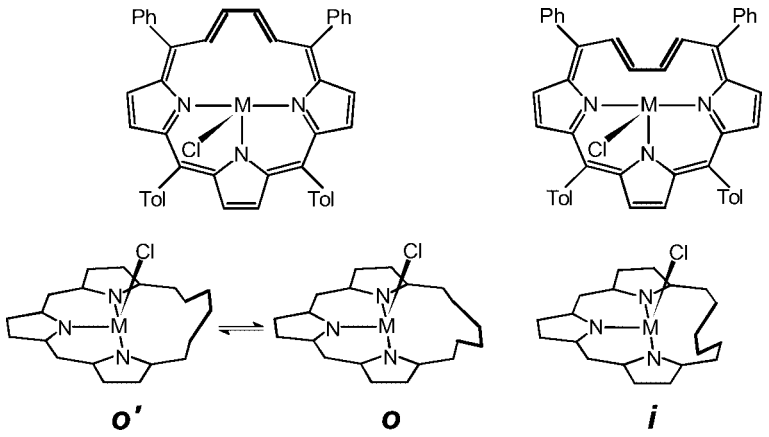

Scheme 5. Stereoisomers of [(VPH_2)Ni^{II}Cl]. Reproduced, with permission, from ref.[73] Copyright 2005 American Chemical Society.

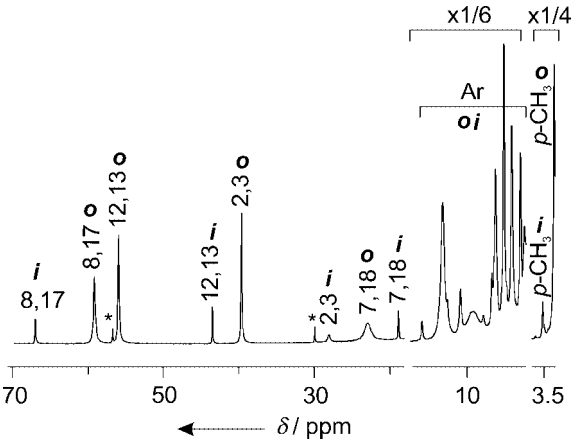

Figure 8. ^{1}H NMR spectra of [(VPH_2)Ni^{II}Cl] ($CDCl_3$, 298 K). The resonances of the different stereoisomers are marked. Reproduced, with permission, from ref.[73] Copyright 2005 American Chemical Society.

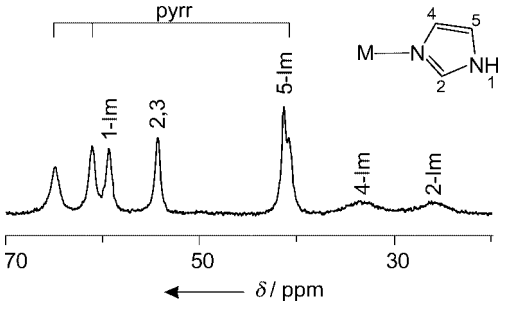

Figure 9. ^{1}H NMR ($CDCl_3$, 298 K) spectra of [(VPH_2)Ni^{II}Cl] in the presence of imidazole. The molar ratio (VPH_2)Ni^{II}Cl/imidazole is 1:2.5. Reproduced, with permission, from ref.[73] Copyright 2005 American Chemical Society.

usual temperature dependence that is characteristic of a dynamic process.[67–69] This behavior can be interpreted in terms of a conformational equilibrium in which one of the forms is present at a very low concentration.[5,61,68] The conformational equilibrium presented in Scheme 5 may contribute to this mechanism providing that the concentration of [(VPH_2)Ni^{II}Cl-*o*] is much greater than that of [(VPH_2)Ni^{II}Cl-*o′*] and that the process is in the slow-exchange limit. Thus, two co-existing stereoisomers reveal a different conformational flexibility in the same solution.

The markedly different spectra of [(VPH_2)Ni^{II}Cl-*i*] in [D_4]MeOH or [D_3]acetonitrile as compared to chlorinated solvents are attributed to an axial coordination of two solvent molecules and formation of a single species, namely [(VPH_2)Ni^{II}(CD_3OD)$_2$]$^+$ or [(VPH_2)Ni^{II}(CD_3CN)$_2$]$^+$. Similarly, the addition of two equivalents of imidazole converts [(VPH_2)Ni^{II}Cl-*o*] and [(VPH_2)Ni^{II}Cl-*i*] into [(VPH_2)-Ni^{II}(Im)$_2$]$^+$ (Figure 9). All resonances of the coordinated imidazole are clearly discernible and have been assigned by line width analysis and selective deuteration. Their positions are similar to those determined for other imidazole adducts of nickel(II) heteroporphyrins.[75]

Iron(II) Complexes of Benziporphyrins

The molecular structure of [(*m*BP*H*)Fe^{II}Br] resembles that of [(*m*BP*H*)Ni^{II}Cl].[65,76] The distances between iron and the pyrrolic nitrogens are in the range for high-spin Fe^{II} porphyrin complexes and the tripyrrolic fragment arranges in a dome-shaped geometry. The distances from iron to the inner C atom [C(22)] and inner hydrogen [H(22)] are 2.579(4) and 2.439(36) Å, respectively. Nevertheless, these values are small compared to the van der Waals contact and suggest the formation of a weak agostic bond.

The β-pyrrolic signals in the ^{1}H NMR spectrum of [(*m*BP*H*)Fe^{II}Br] (Figure 10) are located at δ = 49.4, 21.1, and 6.5 ppm at 298 K, as shown by ^{2}H NMR spectroscopy for [(D_6-*m*BP*H*)Fe^{II}Br].[76] These values are close to those reported for the high-spin nickel(II) complexes [(*m*BP*OAc*)-Ni^{II}Cl] and [(*m*BP*H*)Ni^{II}Cl].[65,66] The hydrogens on the *m*-phenylene ring were identified at δ = 440 [H(22)], 65.8 [H(2,4)], and –33.2 [H(3)] ppm (298 K). An agostic mechanism of spin-density transfer, as described previously for [(*m*BP*H*)Ni^{II}Cl], explains the shifts of [(*m*BP*H*)Fe^{II}Br] as resulting from electron donation from the C–H bond to the metal.

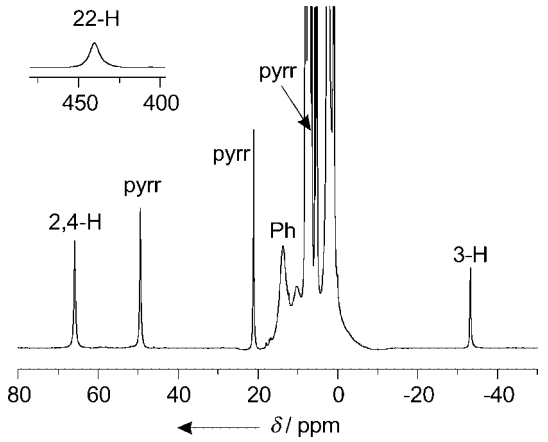

Figure 10. ^{1}H NMR spectrum of [(*m*BP*H*)Fe^{II}Br] (^{1}H NMR, CD_2Cl_2, 298 K). The inset shows the downfield region containing the 22-H resonance. Reproduced, with permission, from ref.[76] Copyright 2004 American Chemical Society.

High-Spin Iron Complexes of *N*-Confused Pyriporphyrin

Insertion of iron(II) into *N*-confused pyriporphyrin, which is the simplest homologue of *N*-confused 5,10,15,20-tetraarylporphyrin, yields the high-spin iron(II) complex [(*N*PyP*H*)Fe^{II}Br] and the diiron species [(Br$_2$LFe^{II}-*N*PyP*H*)Fe^{II}Br] (L = coordinating solvent) where the second iron(II) coordinates to the perimeter nitrogen atom (Scheme 6).[77]

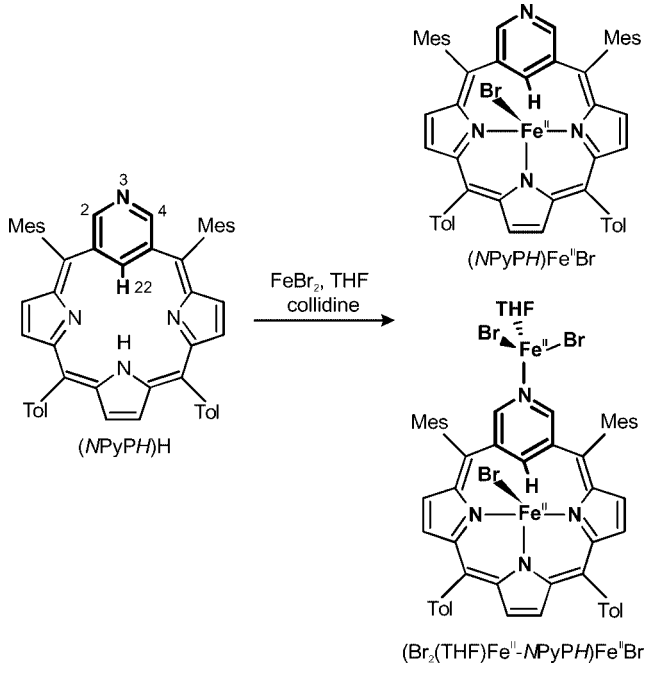

Scheme 6. Synthesis of iron(II) *N*-confused pyriporphyrin complexes. Reproduced, with permission, from ref.[77] Copyright 2006 American Chemical Society.

The characteristic patterns of the pyrrole and pyridine resonances in the ^{1}H NMR spectra were found to be diagnostic of the ground electronic state of iron and the donor properties of C(22)–H and N(3) centers (Figure 11). The downfield H(22) resonances, which are found for iron(II) *N*-confused pyriporphyrin in a very unusual spectroscopic window (δ = 350–800 ppm) for a range of axial ligands, can be considered as a diagnostic sign of an agostic Fe^{II}–{C(22)-H} interaction.[76]

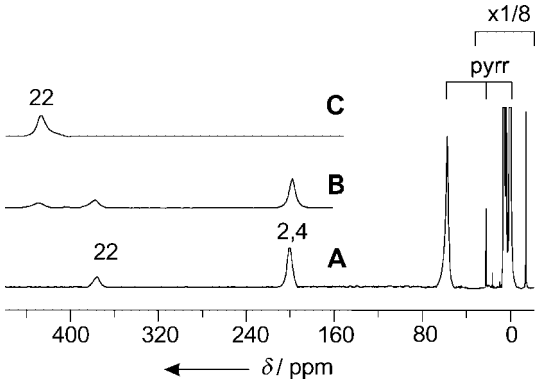

Figure 11. (A) ^{1}H NMR spectrum of [(Br$_2$LFe^{II}-*N*PyP*H*)Fe^{II}Br]; (B) conversion of [(Br$_2$LFe^{II}-*N*PyP)Fe^{II}Br] into [(*N*PyP)Fe^{II}Br] during titration with Br$_2$; (C) [(*N*PyP)Fe^{II}Br]. All spectra were recorded in CD_2Cl_2 at 298 K; L = thf. Reproduced, with permission, from ref.[77] Copyright 2006 American Chemical Society.

To probe the ability of the perimeter nitrogen to bind iron(II) a systematic titration of [(*N*PyP*H*)Fe^{II}Cl] in [D$_3$]-acetonitrile or [D$_8$]THF was carried out. Smooth changes of the chemical shifts of the pyridine moiety directly engaged in coordination were observed during the course of the titration of [(*N*PyP*H*)Fe^{II}Cl] with Fe^{II}Cl$_2$, which was explained by an equilibrium involving a diiron species.

The spectroscopic pattern of [(Br$_2$LFe^{II}-*N*PyP*H*)Fe^{II}Br] in non-coordinating solvents resembles that of the monoiron species [(*N*PyP*H*)Fe^{II}Br], although the H(2,4) resonance is remarkably shifted to δ = 201 ppm (298 K; Figure 11). [(Br$_2$LFe^{II}-*N*PyP)Fe^{II}Br] can be easily converted into [(*N*PyP)Fe^{II}Br] by addition of competing ligands (pyridine) or by an external iron(II)-directed oxidation, which promotes dissociation. In spite of the enormous line widths the far downfield shifted resonances provide an analytically valuable pattern that is unique for the *N*-confused diiron species. The downfield position of the H(2,4) resonance for [(Br$_2$LFe^{II}-*N*PyP)Fe^{II}Br] is consistent with coordination to the high-spin iron(II) assuming that the spin-delocalization pathways are identical to that determined for nickel(II) thiaporphyrin.[78]

Addition of Br$_2$ to a solution of [(*N*PyP*H*)Fe^{II}Br] in the absence of dioxygen results in a one-electron oxidation that yields the high-spin iron(III) *N*-confused pyriporpyrin [(*N*PyP*H*)Fe^{III}Br]$^+$ (Scheme 7). The high-spin complex preserves the side-on interaction between the inverted pyridine ring and iron(III) as in [(*N*PyP*H*)Fe^{II}Br]. The characteristic set of three pyrrole resonances at δ = 122.4, 79.6 and 70.4 ppm ([D$_2$]dichloromethane, 298 K) can be readily assigned to [(*N*PyP)Fe^{III}Br]$^+$. The reaction of [(*N*PyP*H*)-Fe^{II}Br] with dioxygen results in the formation of five-coordinate [(*N*PyPO)Fe^{III}Br] [(*N*PyPO*H*)H = 3-aza-22-hydroxy-*m*-benziporphyrin; Scheme 7].

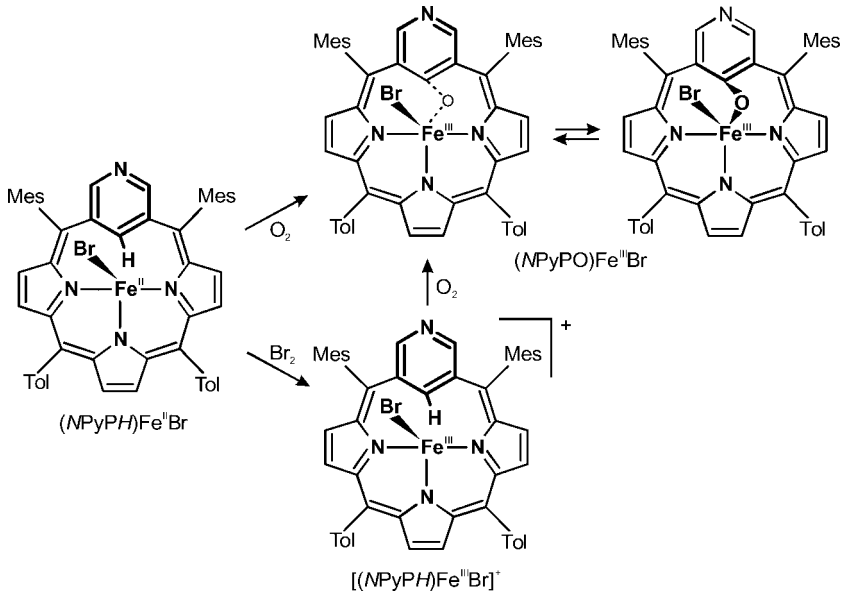

Scheme 7. Oxidation and oxygenation of [(*N*PyPH)Fe^{II}Br]. Reproduced, with permission, from ref.[77] Copyright 2006 American Chemical Society.

Low-Spin Organoiron(III) *N*-Confused Pyriporphyrin

The one-electron oxidation of [(*N*PyPH)Fe^{II}Br] with dioxygen in pyridine, which is accompanied by deprotonation of a C(22)H fragment and formation of an Fe–C(22) bond, produces the low-spin, six-coordinate iron(III) complex [(*N*PyP)Fe^{III}(py)$_2$]$^+$ (Scheme 8), as confirmed by a combination of ^{1}H NMR, EPR and structural data.[79]

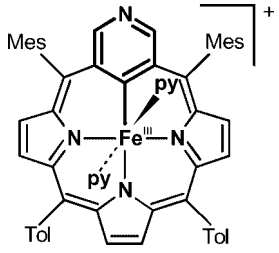

Scheme 8. [(*N*PyP)Fe^{III}(py)$_2$]$^+$.

The cationic complex involves a six-coordinate iron atom bound to the *N*-confused pyriporphyrin through its three pyrrolic nitrogens and the trigonal pyridyl C(22) atom. The porphyrin is strongly ruffled, defining two deep grooves along the C_{meso}–C_{meso} axes that are at right angles to each other. The ^{1}H NMR spectrum of [(PyP)Fe^{III}(D$_5$-py)$_2$]$^+$ is clearly distinct from that of any known low-spin iron(III) porphyrin [β-H: δ = 21.3, 16.2, and 4.1 ppm (CD_2Cl_2, 298 K)]. In fact, only the recently described low-spin iron(III) complex of the "true" pyriporphyrin reveals a similar ^{1}H NMR spectrum.[80] Still, the spectroscopic pattern of the pyrrole and *meso*-aryl resonances is consistent with the features assigned to the less common $(d_{xz}d_{yz})^4(d_{xy})^1$ low-spin ground electronic state.[7,81–83] This unique spectroscopic feature can be related to the extensive ruffling of the macrocycle,[82,84–86] equatorial C-coordination, and/or axial pyridine coordination.[7] A conformational rearrangement process was detected which involves two structures differentiated by macrocyclic ruffling.

Remarkable Paramagnetically Shifted ^{1}H and ^{2}H NMR Spectra of Iron(II) 2-Aza-21-carbaporphyrin

An uncommon type of metal ion–inverted pyrrole ring interaction detected in the solid-state structure of iron(II) 2-aza-21-carbaporphyrin [(*H*CP*H*)Fe^{II}Br] has raised the question of its impact on the ^{1}H NMR spectroscopic features.[87,88] [(*H*CP*H*)Fe^{II}Br] has a conformation where the iron is side-on with respect to the inverted pyrrole plane[87] and the inverted pyrrole ring is sharply bent from the porphyrin plane. The Fe···C(21) distance (2.361 Å) is longer than a regular Fe–C bond but shorter than the sum of the van der Waals radii.

The solid-state geometry of the Fe^{II}···{C(21)–H(21)} fragment in [(*H*CP*H*)Fe^{II}Br] is within the range of an agostic interaction [Fe···H(21) = 1.971 Å].[87] The ^{1}H NMR spectrum of [(*H*CP*H*)Fe^{II}Br] is substantially similar to the spectra of high-spin iron(II) core-modified porphyrins.[14,16,89] Five pyrrole resonances of [(*H*CP*H*)Fe^{II}Br] are spread over the low-field region from δ = 30 to 50 ppm, and two other β-H resonances occur at δ = 8.4 and 0.78 ppm. The resonance at δ = –8.0 ppm (293 K) was assigned to the N(2)H hydrogen. The most characteristic ^{1}H NMR (^{2}H NMR) feature of [(*H*CP*H*)Fe^{II}Br], namely the downfield shifted resonance at δ = 812 ppm (linewidth of 6200 Hz at 293 K in [D$_2$]dichloromethane), was unambiguously assigned to the internal H(21) hydrogen.[88] The ^{2}H NMR spectrum of [(D$_7$-*H*CP*D*)Fe^{II}Br], which stretches over a window of almost 900 ppm, shows the remarkably large paramagnetic shift of C(21)D, as the ^{2}H NMR spectrum

combines simultaneously all pyrrole resonances, including the C(21)D one (Figure 12). Variable-temperature NMR measurements for the C(21)H resonance of [(*H*CP*H*)Fe^{II}Br] revealed remarkable changes of the chemical shifts, which fall in a window of 1244 ppm at 208 K. Addition of 2-methylimidazole to a [D_2]dichloromethane solution of [(*H*CP*H*)Fe^{II}Br] results in the formation of the high-spin five-coordinate species [(*H*CP*H*)Fe^{II}(2-MeIm)]$^+$, which was identified by the unique chemical shift of the C(21)H resonance (δ = 1090 ppm). To the best of our knowledge these are the largest chemical shifts reported thus far for iron porphyrins or iron porphyrin derivatives[7,90,91] and are even larger than the extreme chemical shifts determined for paramagnetic compounds, including σ-aryl complexes of nickel(II) heteroporphyrins (e.g. *ortho*-H: δ = 568 ppm at 203 K).[6,39,78,92] Extreme contact shifts have been reported for the β-CH_2 hydrogens of cysteines that ligate iron in oxidized ruberodoxin (δ = 300–900 ppm, 303 K)[93] and copper(II) in azurin (δ = 800, 850 ppm at 278 K).[94]

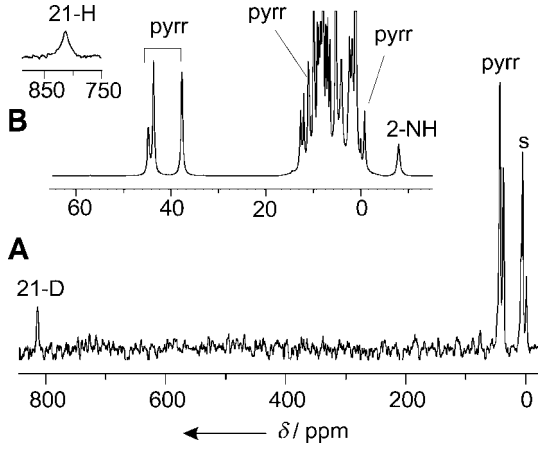

Figure 12. (A) ^{2}H NMR spectrum of [(D_7-*H*CP*D*)Fe^{II}Br] (CH_2Cl_2, 298 K). (B) ^{1}H NMR spectrum of [(*H*CP*H*)Fe^{II}Br] (CD_2Cl_2, 298 K); s: solvent. The inset in (B) shows the H(21) resonance. Reproduced, with permission, from ref.[88] Copyright 2003 American Chemical Society.

The ^{1}H NMR spectra of iron(II) 2-aza-21-carbaporphyrins display the spread of regular β-H resonances, which is markedly larger than for their more symmetrical counterparts.[11,89,95] The paramagnetic shifts of [(*H*CP*H*)Fe^{II}Br] can be explained by a model that is typically applied to high-spin iron(II) porphyrins and iron(II) *N*-substituted porphyrins. In the case of a high-spin iron(II) center [$(d_{xy})^2(d_{xz}d_{yz})^2(d_{z^2})^1(d_{x^2-y^2})^1$] both σ and π routes of spin density delocalization can operate. The contact shift predominates for the regular pyrrole resonances, which determines their downfield positions.[7,14,16] The typical delocalization pathways involve delocalization through a σ-framework by way of σ-donation to the half occupied $d_{x^2-y^2}$ iron(II) orbital.[14] Actually, the variation of the β-H positions in the ^{1}H NMR spectrum may be accounted for by specific π-delocalization mechanisms that have been discussed in detail for iron(III) porphyrins.[96,97] One pyrrole 3-H and the 2-NH resonance are evidently different from the other six and show upfield shifts. Thus, the side-on location of the iron(II) with respect to the pyrrole ring primarily affects spin transfer to the modified pyrrole ring. An analogous effect has been observed for paramagnetic nickel(II) 2-aza-21-carbaporphyrin and metalloheteroporphyrins.[39,52] Significantly, the peculiar metal ion–inverted pyrrole ring interaction detected in the solid-state structure of [(*H*CP*H*)Fe^{II}Br] is clearly reflected by an unprecedented isotropic shift of the H(21) atom that is involved in an agostic interaction [Fe^{II}–C(21)H] in solution.

Oxidation and Oxygenation of Iron(II) 2-Aza-21-carbaporphyrin

Dioxygen reacts cleanly with iron(II) 2-aza-21-carbaporphyrin to form the corresponding five-coordinate intermediate-spin iron(III) complexes and, eventually, the 2-aza-21-carbaporphyrin gains an oxo functionality.[98] Generally speaking insertion of an oxygen atom into an M–C bond (a carbon atom built into the aromatic moiety) is quite rare,[99–109] and no direct evidence for the formation of intermediates in the oxygenation process has been found.

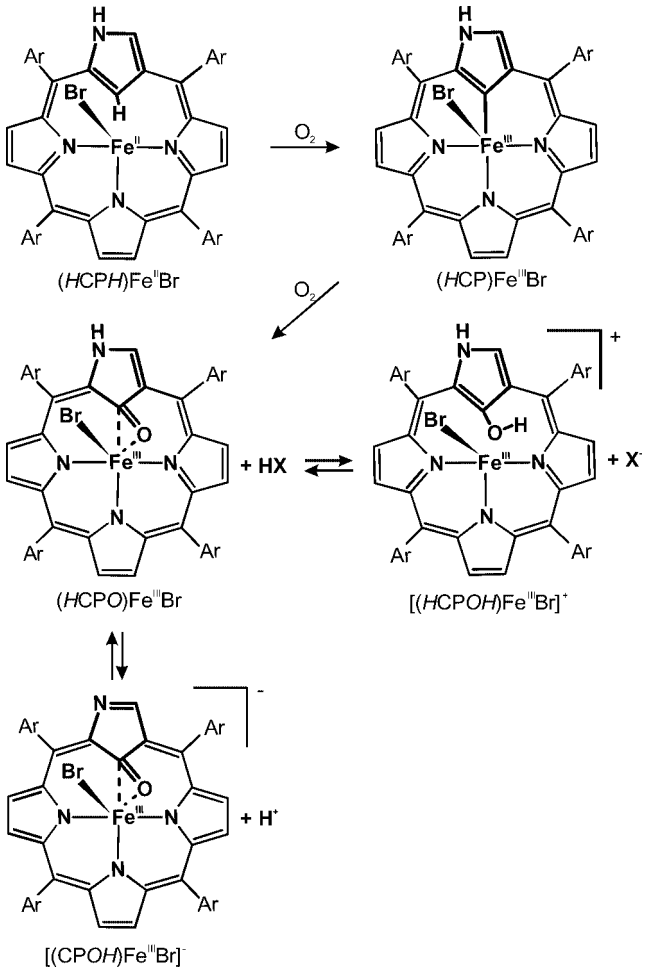

Scheme 9. Reaction of [(*H*CP*H*)Fe^{II}Br] with dioxygen. Reproduced, with permission, from ref.[98] Copyright 2004 American Chemical Society.

The oxidation and oxygenation of [(*H*CP*H*)Fe^{II}Br] have been followed by ^{1}H and ^{2}H NMR spectroscopy.[98] Thus, addition of dioxygen to [(*H*CP*H*)Fe^{II}Br] in dichloromethane yields a series of iron(III) complexes in consecutive reactions (Scheme 9).

One-electron oxidation with dioxygen, which is accompanied by deprotonation of a C(21)H fragment and formation of an Fe–C(21) bond, produces the intermediate-spin, five-coordinate iron(III) complex [(*H*CP)Fe^{III}Br] (Scheme 10). Insertion of an oxygen atom into the preformed Fe^{III}–C(21) bond in the subsequent step yields [(*H*CP*O*)Fe^{III}Br]. Protonation at the oxygen atom then affords [(*H*CP*OH*)$Fe^{III}Br]^+$. The considered mechanism of [(*H*CP)Fe^{III}Br] oxygenation involves the insertion of dioxygen into the Fe–C bond. The O–O bond of the transient species cleaves rapidly and 2-aza-carbaporphyrin acquires an oxo functionality [C(21)O] in the coordination core.

Addition of I_2 or Br_2 to a solution of [(*H*CP*H*)Fe^{II}Br] in the absence of dioxygen results in a one-electron oxidation that yields [(*H*CP*H*)$Fe^{III}Br]^+$. This iron(III) compound has also been obtained by titration of [(*H*CP)Fe^{III}Br] with acids due to protonation at C(21). Addition of Br_2 to a solution containing [(*H*CP)Fe^{III}Br] or [(*H*CP*H*)$Fe^{III}Br]^+$ results in bromination at C(21) to yield [(*H*CP*Br*)$Fe^{III}Br]^+$, in agreement with the typical reactivity of inverted porphyrins.[51,110] Subsequent reaction with water results finally in formation of the C=O fragment in [(*H*CP*O*)Fe^{III}Br]. This complex contains a ligand which is a 2-aza-21-carbaporphyrin derivative with the oxygen atom located on the inner carbon, in other words *N*-confused porphyrin *C*-oxide. Such a ligand was first detected in the dimeric product of [{(CP*H*)Fe^{II}}$_2$] oxygenation, although in a different tautomeric form,[111] and in the oxidation of [(*H*CPH)Ni^{II}] with OsO_4.[112]

Selected spectra that emphasize the utility of ^{1}H NMR spectroscopy for observing oxidation/oxygenation transformations of [(*H*CP*H*)Fe^{II}Br] are presented in Figure 13. The characteristic patterns of pyrrole and N(2)H resonances are diagnostic of the ground electronic state of iron and the donor character of C(21).

The average chemical shift of the perimeter resonances (δ_{av}) at 298 K was considered here as a suitable parameter for characterizing the ground electronic/spin state of iron(*n*) inverted porphyrins. Thus, the value of δ_{av} for six regular pyrroles was examined for [(*H*CP*H*)Fe^{II}Br], [(*H*CP*H*)-$Fe^{III}Br]^+$, and [(*H*CP*Br*)$Fe^{III}Br]^+$, where a side-on location of the metal ion with respect to the *N*-confused pyrrole ring has been determined. The values of δ_{av} for [(*H*CP*O*)-Fe^{III}Br], [(*H*CP*OH*)$Fe^{III}Br]^+$, [(*H*CP*H*)$Fe^{III}Br]^+$, and [(*H*CP*Br*)$Fe^{III}Br]^+$ approach those found for high-spin iron(III) tetraarylporphyrins,[7] iron(III) β-substituted tetraarylporphyrin,[96] and iron(III) *N*-methyltetraarylporphyrin (δ_{av} for regular pyrrole rings),[13] and the average chemical shift of [(*H*CP*H*)Fe^{II}Br] is consistent with that found for high-spin iron(II) tetraarylporphyrins, iron(II) *N*-methyltetraarylporphyrin, and iron(II) 21-thiatetraarylporphyrin.[7,14,89] Finally, the upfield β-H positions seen for [(*H*CP)Fe^{III}Br] and [(*H*CP)Fe^{III}(1-MeIm)]$_2^+$ are clearly consistent with intermediate- and low-spin states, respectively, considering the asymmetric iron(III) porphyrins as reference molecules.[7,11,95,113,114]

The isotropic shift pattern for the β-H pyrrole of [(*H*CP)-Fe^{III}Br] and [(*H*CP)Fe^{III}(1-MeIm)]$_2^+$ reflects the extensive spin delocalization into the π molecular orbitals of the in-

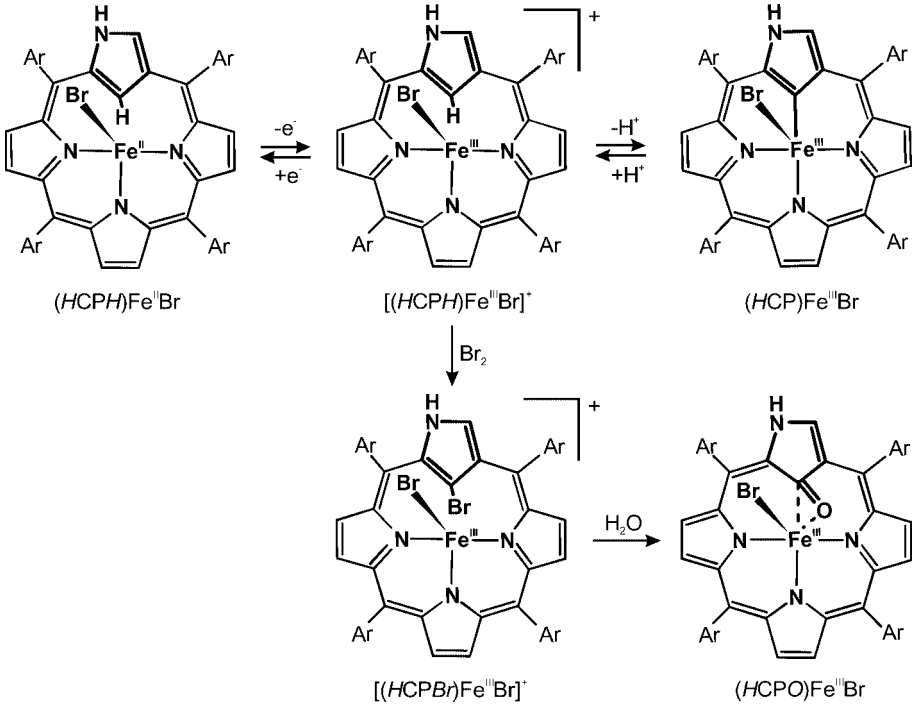

Scheme 10. Oxidation of [(*H*CP*H*)Fe^{II}Br]. Reproduced, with permission, from ref.[98] Copyright 2004 American Chemical Society.

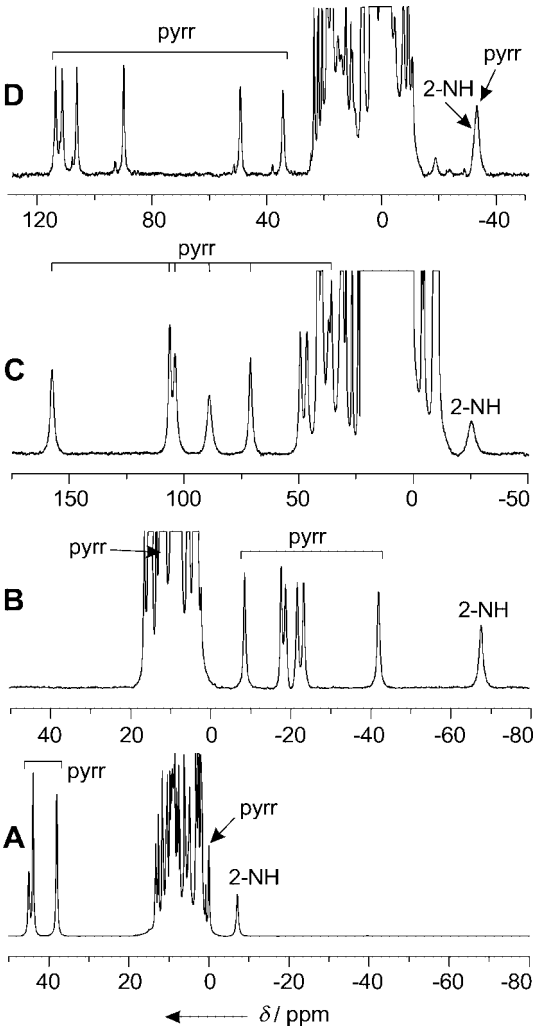

Figure 13. Oxidation and oxygenation of iron inverted porphyrins as followed by ^{1}H NMR spectroscopy (CD_2Cl_2, 298 K): (A) [(*H*CP*H*)Fe^{II}Br]; (B) [(*H*CP)Fe^{III}Br]; (C) ([*H*CP*O*)Fe^{III}Br]; (D) [(*H*CP*H*)Fe^{III}Br]$^+$. Reproduced, with permission, from ref.[98] Copyright 2004, American Chemical Society.

verted porphyrin. The dominance of the π-spin transfer mechanism has been taken as direct evidence that $d_{x^2-y^2}$ is not populated in [(*H*CP)Fe^{III}Br] and [(*H*CP)Fe^{III}-(1-MeIm)]$_2^+$. Thus, the ground state can be related to the following models of the electronic configuration: intermediate-spin $(d_{xy})^2(d_{xz})^1(d_{yz})^1(d_{z^2})^1(d_{x^2-y^2})^0$ for [(*H*CP)Fe^{III}Br] and low-spin $(d_{xy})^2(d_{xz}d_{yz})^3(d_{z^2})^0(d_{x^2-y^2})^0$ for [(*H*CP)Fe^{III}-(1-MeIm)]$_2^+$. The β-H shifts of [(*H*CP)Fe^{III}Br] are larger as there are two π-symmetry unpaired electrons in the S = 3/2 state in comparison to one π electron in [(*H*CP)Fe^{III}-(1-MeIm)]$_2^+$ (S = 1/2).[113]

An extension of these investigations to *N*- and *C*-methylated iron porphyrins allowed the similarities of iron(*n*) *N*-confused and *C*- and *N*-methylated *N*-confused porphyrin complexes for a given oxidation/spin state to be established.[115] There are considerable similarities in the ^{1}H NMR properties within each of these pairs. The analytically useful hyperfine shift patterns determined previously for iron(II) and iron(III) *N*-confused porphyrin provided useful and potentially unique probes for detecting the analogous species by ^{1}H NMR spectroscopy. This spectroscopic means of identification has gained an additional advantage, namely the characteristic large downfield C-*Me* contact shift provides a well-defined signal in a unique window (δ = 420–520 ppm) for iron(III) *C*-methylated *N*-confused porphyrins, which contrasts with the relatively small values for iron(II) *C*-methylated derivatives (δ = 50–80 ppm). The most characteristic ^{1}H NMR features of [(*H*CP*Me*)-Fe^{III}Br]$^+$ and [(*Me*CP*Me*)Fe^{III}Br]$^+$, namely the broad resonances at δ = 498 or 432 ppm, can be assigned to the internal C-*Me* groups. The directions and magnitudes of these shifts resemble those reported for the N-*Me* group of the [(*Me*TPP)Fe^{III}Cl]$^+$ complex.[13]

Dioxygen reacts cleanly with the carbaporphyrin complex [(*Me*CP*H*)Fe^{II}Br] to form the corresponding five-coordinate intermediate-spin iron(III) complex [(*Me*CP)Fe^{III}Br] although, contrary to 2-aza-21-carbaporphyrin, the *N*-methylated derivative does not acquire an oxo functionality. Similarly, the C-*Me* group, which is positioned near the center of the carbaporphyrin, presents a serious steric barrier that plays an essential role in governing the reactivity of this iron *C*-methylated *N*-confused porphyrin. For instance, [(*Me*CP*Me*)Fe^{II}Br] undergoes only one-electron oxidation. Further investigations of the iron carbaporphyrinoid complexes are expected to afford a unique insight into the reactivity of a metal–C bond as specifically tuned carbaporphyrins can be expected to influence feasible pathways of oxygenation processes.

Conclusions

In a sense, in this microreview we have intended to remind the community of inorganic chemists that NMR of paramagnetic molecules can be considered as a powerful spectroscopic probe of intriguing aspects of molecular and electronic structures, structural rearrangements, and reactivity. The chosen examples address the chemistry of a new class of carbaporphyrinoid complexes that has recently been explored in our laboratory. As presented, the entrapment of metal ions in the coordination core of carbaporphyrinoids creates a very efficient protection of the metal–C bond and allows the stabilization of extremely rare or virtually unknown oxidation/electronic states of metal ions in an organometallic environment, such as copper(II),[63,116,117] silver(III),[118,119] iron(III),[98] or paramagnetic nickel(II).[44,52] Extensive studies on the NMR of paramagnetic metallocarbaporphyrinoids (reviewed above) have established a general relationship between the isotropic shift pattern of these porphyrin-like macrocycles and their electronic and molecular structures. In particular, we have found that the restraints introduced by incorporating the carbocyclic moiety into an appropriately sized carbaporphyrinoid allow the creation of a geometry that affords metal–carbocyclic ring distances that can be classified as intermediate between a regular chemical bond and a van der Waals interaction.[57,65,67,76] The proximity of a dia-

magnetic metal ion and an arene gives rise to observable ^{1}H-M and ^{13}C-M scalar couplings in the NMR spectra (M = NMR-active metal ion). Such couplings are usually classified as "through-space" or "nonbonding" because their magnitude cannot be rationalized in terms of the network of regular bonds in the molecule.[57,65,120] The metal–arene interactions of nickel(II), iron(II), and iron(III) have been probed in complementary investigations using their paramagnetically shifted ^{1}H NMR spectra.[52,65,76,88,98] NMR spectroscopy provides a uniquely useful probe for studying this type of interaction. Apart from purely structural considerations, the understanding of such a "borderline" M···C–H interaction is fundamental for the exploration of transient states that might be active in organometallic catalysis.

Acknowledgments

Financial support from the Ministry of Science and Higher Education (grant no. 3 T09A 162 28) is gratefully acknowledged.

[1] *NMR of Paramagnetic Molecules. Principles and Applications* (Eds.: G. N. La Mar, W. DeWitt Horrocks Jr, R. H. Holm), Academic Press, New York, **1973**.
[2] G. N. La Mar, F. A. Walker, *NMR of Paramagnetic Porphyrins*, in *The Porphyrins* (Ed.: D. Dolphin), Academic Press, New York, **1979**, p. 57.
[3] F. A. Walker, U. Simonis, N*MR of Paramagnetic Molecules*, in *Biological Magnetic Resonance* (Eds.: L. J. Berliner, S. Reuben), Plenum Press, New York, **1993**, p. 133.
[4] *NMR of Paramagnetic Molecules* (Eds.: L. J. Berliner, J. Reuben), Plenum Press, New York, **1993**.
[5] I. Bertini, C. Luchinat, *Coord. Chem. Rev.* **1996**, *150*, 1.
[6] F. A. Walker, *Advances in Single- and Multidimensional NMR Spectroscopy of Paramagnetic Metal Complexes*, in *Spectroscopic Methods in Bioinorganic Chemistry; ACS Symposium Books* (Eds.: E. I. Solomon, K. Hodgson), American Chemical Society, Washington, D. C., **1998**, p. 30.
[7] F. A. Walker, *Proton NMR and EPR Spectroscopy of Paramagnetic Metalloporphyrins*, in *The Porphyrin Handbook* (Eds.: K. M. Kadish, K. M. Smith, R. Guilard), Academic Press, San Diego, CA, **2000**, p. 81.
[8] G. N. La Mar, J. D. Satterlee, J. S. De Ropp, *Nuclear Magnetic Resonance of Hemoproteins*, in *The Porphyrin Handbook* (Eds.: K. M. Kadish, K. M. Smith, R. Guilard), Academic Press, San Diego, CA, **2000**, p. 185.
[9] I. Bertini, C. Luchinat, G. Parigi, *Solution NMR of Paramagnetic Molecules, Application to Metallobiomolecules and Models*, vol. 2, *Current Methods in Inorganic Chemistry*, Elsevier, Amsterdam, **2001**.
[10] F. A. Walker, *Inorg. Chem.* **2003**, *42*, 4526.
[11] A. L. Balch, C. R. Cornman, L. Latos-Grażyński, M. M. Olmstead, *J. Am. Chem. Soc.* **1990**, *112*, 7552.
[12] A. L. Balch, C. R. Cornman, L. Latos-Grażyński, M. W. Renner, *J. Am. Chem. Soc.* **1992**, *114*, 2230.
[13] A. L. Balch, G. N. La Mar, L. Latos-Grażyński, M. W. Renner, *Inorg. Chem.* **1985**, *24*, 2432.
[14] A. L. Balch, Y.-W. Chan, G. N. La Mar, L. Latos-Grażyński, M. W. Renner, *Inorg. Chem.* **1985**, *24*, 1437.
[15] A. Wysłouch, L. Latos-Grażyński, M. Grzeszczuk, K. Drabent, T. Bartczak, *J. Chem. Soc., Chem. Commun.* **1988**, 1377.
[16] M. Pawlicki, L. Latos-Grażyński, *Inorg. Chem.* **2002**, *41*, 5866.
[17] M. Pawlicki, L. Latos-Grażyński, *Inorg. Chem.* **2004**, *43*, 5564.
[18] P. J. Chmielewski, L. Latos-Grażyński, M. M. Olmstead, A. L. Balch, *Chem. Eur. J.* **1997**, *3*, 268.
[19] P. J. Chmielewski, L. Latos-Grażyński, *Inorg. Chem.* **1998**, *37*, 4179.
[20] L. Banci, I. Bertini, C. Luchinat, P. Turano, *Solution Structures of Hemoproteins*, in *The Porphyrin Handbook* (Eds.: K. M. Kadish, K. M. Smith, R. Guilard), Academic Press, San Diego, CA, **2000**, p. 323.
[21] A. L. Balch, Y.-W. Chan, R.-J. Cheng, G. N. La Mar, L. Latos-Grażyński, M. W. Renner, *J. Am. Chem. Soc.* **1984**, *106*, 7779.
[22] A. L. Balch, L. Latos-Grażyński, M. W. Renner, *J. Am. Chem. Soc.* **1985**, *107*, 2983.
[23] K. Rachlewicz, L. Latos-Grażyński, E. Vogel, *Inorg. Chem.* **2000**, *39*, 3247.
[24] A. L. Balch, L. Latos-Grażyński, B. C. Noll, M. M. Olmstead, N. Safari, *J. Am. Chem. Soc.* **1993**, *115*, 9056.
[25] A. L. Balch, L. Latos-Grażyński, B. C. Noll, M. M. Olmstead, L. Szterenberg, E. P. Zovinka, *J. Am. Chem. Soc.* **1993**, *115*, 11846.
[26] A. L. Balch, L. Latos-Grażyński, T. N. St. Claire, *Inorg. Chem.* **1995**, *34*, 1395.
[27] A. L. Balch, R. Koerner, L. Latos-Grażyński, B. C. Noll, *J. Am. Chem. Soc.* **1996**, *118*, 2760.
[28] A. L. Balch, R. Koerner, L. Latos-Grażyński, J. E. Lewis, T. N. St. Claire, E. P. Zovinka, *Inorg. Chem.* **1997**, *36*, 3892.
[29] R. Koerner, L. Latos-Grażyński, A. L. Balch, *J. Am. Chem. Soc.* **1998**, *120*, 9246.
[30] H. Kalish, L. Latos-Grażyński, A. L. Balch, *J. Am. Chem. Soc.* **2000**, *122*, 12478.
[31] H. Kalish, J. E. Camp, M. Stępień, L. Latos-Grażyński, A. L. Balch, *J. Am. Chem. Soc.* **2001**, *123*, 11719.
[32] H. Kalish, J. E. Camp, M. Stępień, L. Latos-Grażyński, M. M. Olmstead, A. L. Balch, *Inorg. Chem.* **2002**, *41*, 989.
[33] L. Szterenberg, L. Latos-Grażyński, J. Wojaczyński, *ChemPhysChem.* **2003**, *4*, 691.
[34] H. Kalish, H. M. Lee, M. M. Olmstead, L. Latos-Grażyński, S. P. Rath, A. L. Balch, *J. Am. Chem. Soc.* **2003**, *125*, 4674.
[35] K. T. Nguyen, S. P. Rath, L. Latos-Grażyński, M. M. Olmstead, A. L. Balch, *J. Am. Chem. Soc.* **2004**, *126*, 6210.
[36] P. J. Chmielewski, L. Latos-Grażyński, K. Rachlewicz, T. Głowiak, *Angew. Chem. Int. Ed. Engl.* **1994**, *33*, 779.
[37] H. Furuta, T. Asano, T. Ogawa, *J. Am. Chem. Soc.* **1994**, *116*, 767.
[38] T. D. Lash, *Synlett* **1999**, 279.
[39] L. Latos-Grażyński, *Core Modified Heteroanalogues of Porphyrins and Metalloporphyrins*, in *The Porphyrin Handbook* (Eds.: K. M. Kadish, K. M. Smith, R. Guilard), Academic Press, New York, **2000**, p. 361.
[40] H. Furuta, H. Maeda, A. Osuka, *Chem. Commun.* **2002**, 1795.
[41] J. D. Harvey, C. J. Ziegler, *Coord. Chem. Rev.* **2003**, *247*, 1.
[42] A. Ghosh, *Angew. Chem. Int. Ed.* **2004**, *43*, 1918.
[43] A. Srinivasan, H. Furuta, *Acc. Chem. Res.* **2005**, *38*, 10.
[44] P. J. Chmielewski, L. Latos-Grażyński, *Coord. Chem. Rev.* **2005**, *249*, 2510.
[45] M. Stępień, L. Latos-Grażyński, *Acc. Chem. Res.* **2005**, *38*, 88.
[46] F.-P. Monforts, M. Glasenapp-Breiling, D. Kusch, *Porphyrins and Related Compounds*, in *Hetarenes*, Thieme, Stuttgart, New York, **1998**, p. 577.
[47] J. L. Sessler, A. Gebauer, E. Vogel, *Porphyrin Isomers*, in *The Porphyrin Handbook* (Eds.: K. M. Kadish, K. M. Smith, R. Guilard), Academic Press, San Diego, CA, **2000**, p. 1.
[48] K. Berlin, E. Breitmaier, *Angew. Chem. Int. Ed. Engl.* **1994**, *33*, 1246.
[49] T. D. Lash, *Angew. Chem. Int. Ed. Engl.* **1995**, *34*, 2533.
[50] T. D. Lash, *Syntheses of Novel Porphyrinoid Chromophores*, in *The Porphyrin Handbook* (Eds.: K. M. Kadish, K. M. Smith, R. Guilard), Academic Press, San Diego, CA, **2000**, p. 125.
[51] P. J. Chmielewski, L. Latos-Grażyński, *J. Chem. Soc., Perkin Trans. 2* **1995**, 503.
[52] P. J. Chmielewski, L. Latos-Grażyński, T. Głowiak, *J. Am. Chem. Soc.* **1996**, *118*, 5690.
[53] I. Schmidt, P. J. Chmielewski, *Tetrahedron Lett.* **2001**, *42*, 6389.

[54] I. Schmidt, P. J. Chmielewski, *Inorg. Chem.* **2003**, *42*, 5579.
[55] I. Schmidt, P. J. Chmielewski, Z. Ciunik, *J. Org. Chem.* **2002**, *67*, 8917.
[56] M. Stępień, L. Latos-Grażyński, *Chem. Eur. J.* **2001**, *7*, 5113.
[57] M. Stępień, L. Latos-Grażyński, *J. Am. Chem. Soc.* **2002**, *124*, 3838.
[58] E. Pacholska, L. Latos-Grażyński, Z. Ciunik, *Chem. Eur. J.* **2002**, *8*, 5403.
[59] R. Myśliborski, L. Latos-Grażyński, *Eur. J. Org. Chem.* **2005**, 5039.
[60] P. J. Chmielewski, L. Latos-Grażyński, *Inorg. Chem.* **1997**, *36*, 840.
[61] T. J. Swift, *The Paramagnetic Linewidth*, in *NMR of Paramagnetic Molecules. Principles and Applications* (Eds.: G. N. La Mar, W. D. Holm Jr, R. H. Horrocks), Academic Press, New York, **1973**, p. 53.
[62] P. J. Chmielewski, L. Latos-Grażyński, *Inorg. Chem.* **2000**, *39*, 5639.
[63] P. J. Chmielewski, L. Latos-Grażyński, I. Schmidt, *Inorg. Chem.* **2000**, *39*, 5475.
[64] G. Mitrikas, C. Calle, A. Schweiger, *Angew. Chem. Int. Ed.* **2005**, *44*, 3301.
[65] M. Stępień, L. Latos-Grażyński, L. Szterenberg, J. Panek, Z. Latajka, *J. Am. Chem. Soc.* **2004**, *126*, 4566.
[66] M. Stępień, L. Latos-Grażyński, *Inorg. Chem.* **2003**, *42*, 6183.
[67] M. Stępień, L. Latos-Grażyński, L. Szterenberg, *Inorg. Chem.* **2004**, *43*, 6654.
[68] J. D. Satterlee, G. N. La Mar, T. J. Bold, *J. Am. Chem. Soc.* **1977**, *99*, 1088.
[69] G. N. La Mar, E. O. Sherman, *J. Am. Chem. Soc.* **1970**, *92*, 2691.
[70] K. M. Barkigia, M. D. Berber, C. J. Medforth, M. W. Renner, K. M. Smith, *J. Am. Chem. Soc.* **1990**, *112*, 8851.
[71] C. J. Medforth, *NMR Spectroscopy of Diamagnetic Porphyrins*, in *The Porphyrin Handbook* (Eds.: K. M. Kadish, K. M. Smith, R. Guilard), Academic Press, San Diego, CA, **2000**, p. 1.
[72] C. J. Medforth, M. D. Berber, K. M. Smith, J. A. Shelnutt, *Tetrahedron Lett.* **1990**, *31*, 3719.
[73] E. Pacholska-Dudziak, J. Skonieczny, M. Pawlicki, L. Latos-Grażyński, L. Szterenberg, *Inorg. Chem.* **2005**, *44*, 8794.
[74] J. Lisowski, L. Latos-Grażyński, L. Szterenberg, *Inorg. Chem.* **1992**, *31*, 1933.
[75] L. Latos-Grażyński, E. Pacholska, P. J. Chmielewski, M. M. Olmstead, A. L. Balch, *Inorg. Chem.* **1996**, *35*, 566.
[76] C.-H. Hung, F.-C. Chang, C.-Y. Lin, K. Rachlewicz, M. Stępień, L. Latos-Grażyński, G.-H. Lee, S.-M. Peng, *Inorg. Chem.* **2004**, *43*, 4118.
[77] R. Myśliborski, K. Rachlewicz, L. Latos-Grażyński, *Inorg. Chem.* **2006**, *45*, 7828.
[78] P. J. Chmielewski, L. Latos-Grażyński, *Inorg. Chem.* **1992**, *31*, 5231.
[79] R. Myśliborski, K. Rachlewicz, L. Latos-Grażyński, *J. Porphyrins Phthalocyanines* **2007**, in press.
[80] R. Myśliborski, L. Latos-Grażyński, L. Szterenberg, *Eur. J. Org. Chem.* **2006**, 3064.
[81] G. Simonneaux, F. Hindre, M. Le Plouzennec, *Inorg. Chem.* **1989**, *28*, 823.
[82] S. Wołowiec, L. Latos-Grażyński, M. Mazzanti, J.-C. Marchon, *Inorg. Chem.* **1997**, *36*, 5761.
[83] S. Wołowiec, L. Latos-Grażyński, D. Toronto, J.-C. Marchon, *Inorg. Chem.* **1998**, *37*, 724.
[84] M. Nakamura, T. Ikeue, H. Fujii, T. Yoshimura, *J. Am. Chem. Soc.* **1997**, *119*, 6284.
[85] T. Ikeue, Y. Ohgo, T. Saitoh, T. Yamaguchi, M. Nakamura, *Inorg. Chem.* **2001**, *40*, 3423.
[86] H. Ogura, L. Yatsunyk, C. J. Medforth, K. M. Smith, K. M. Barkigia, M. W. Renner, D. Melamed, F. A. Walker, *J. Am. Chem. Soc.* **2001**, *123*, 6564.
[87] W.-C. Chen, C.-H. Hung, *Inorg. Chem.* **2001**, *40*, 5070.
[88] K. Rachlewicz, S.-L. Wang, C.-H. Peng, C.-H. Hung, L. Latos-Grażyński, *Inorg. Chem.* **2003**, *42*, 7348.
[89] L. Latos-Grażyński, J. Lisowski, M. M. Olmstead, A. L. Balch, *Inorg. Chem.* **1989**, *28*, 1183.
[90] Z. Li, H. M. Goff, *Inorg. Chem.* **1992**, *31*, 1548.
[91] L. Latos-Grażyński, J. Wojaczyński, R. Koerner, J. J. Johnson, A. L. Balch, *Inorg. Chem.* **2001**, *40*, 4971.
[92] C. Luchinat, S. Steuernagel, P. Turano, *Inorg. Chem.* **1990**, *29*, 4351.
[93] B. Xia, W. M. Westler, H. Cheng, J. Meyer, J.-M. Moulis, J. L. Markley, *J. Am. Chem. Soc.* **1995**, *117*, 5347.
[94] I. Bertini, C. O. Fernández, B. G. Karlsson, J. Leckner, C. Luchinat, B. G. Malmström, A. M. Nersissian, R. Pierattelli, E. Ship, J. S. Valentine, A. J. Vila, *J. Am. Chem. Soc.* **2000**, *122*, 3701.
[95] A. L. Balch, R.-J. Cheng, G. N. La Mar, L. Latos-Grażyński, *Inorg. Chem.* **1985**, *24*, 2651.
[96] J. Wojaczyński, L. Latos-Grażyński, W. Hrycyk, E. Pacholska, K. Rachlewicz, L. Szterenberg, *Inorg. Chem.* **1996**, *35*, 6861.
[97] R.-J. Cheng, P.-Y. Chen, T. Lovell, T. Liu, L. Noodleman, D. A. Case, *J. Am. Chem. Soc.* **2003**, *125*, 6774.
[98] K. Rachlewicz, S.-L. Wang, J.-L. Ko, C.-H. Hung, L. Latos-Grażyński, *J. Am. Chem. Soc.* **2004**, *126*, 4420.
[99] B. A. Grigor, A. Neilson, *J. Organomet. Chem.* **1977**, *129*, C17.
[100] K. Kamaraj, D. Bandyopadhyay, *J. Am. Chem. Soc.* **1997**, *119*, 8099.
[101] P. Wadhwani, M. Mukherjee, D. Bandyopadhyay, *J. Am. Chem. Soc.* **2001**, *123*, 12430.
[102] A. D. Ryabov, *Synthesis* **1985**, 233.
[103] A. K. Mahapatra, D. Bandyopadhyay, P. Bandyopadhyay, A. Chakravorty, *Inorg. Chem.* **1986**, *25*, 2214.
[104] C. Sinha, D. Bandyopadhyay, A. Chakravorty, *Inorg. Chem.* **1988**, *27*, 1173.
[105] S. Chattopadhyay, C. Sinha, P. Basu, A. Chakravorty, *Organometallics* **1991**, *10*, 1135.
[106] A. Marsella, S. Agapakis, F. Pinna, G. Strukul, *Organometallics* **1992**, *11*, 3578.
[107] J.-M. Valk, J. Boersma, G. van Koten, *Organometallics* **1996**, *15*, 4366.
[108] R. D. Arasasingham, A. L. Balch, R. H. Hart, L. Latos-Grażyński, *J. Am. Chem. Soc.* **1990**, *112*, 7566.
[109] A. L. Balch, R. H. Hart, L. Latos-Grażyński, *Inorg. Chem.* **1990**, *29*, 3253.
[110] H. Furuta, T. Ishizuka, A. Osuka, T. Ogawa, *J. Am. Chem. Soc.* **1999**, *121*, 2945.
[111] C.-H. Hung, W.-C. Chen, G.-H. Lee, S.-M. Peng, *Chem. Commun.* **2002**, 1516.
[112] Z. Xiao, B. O. Patrick, D. Dolphin, *Inorg. Chem.* **2003**, *42*, 8125.
[113] J.-P. Simonato, J. Pécaut, L. Le Pape, J.-L. Oddou, C. Jeandey, M. Shang, W. R. Scheidt, J. Wojaczyński, S. Wołowiec, L. Latos-Grażyński, J.-C. Marchon, *Inorg. Chem.* **2000**, *39*, 3978.
[114] K. Rachlewicz, L. Latos-Grażyński, E. Vogel, Z. Ciunik, L. Jerzykiewicz, *Inorg. Chem.* **2002**, *41*, 1979.
[115] K. Rachlewicz, D. Gorzelańczyk, L. Latos-Grażyński, *Inorg. Chem.* **2006**, *45*, 9742.
[116] H. Furuta, T. Ishizuka, A. Osuka, Y. Uwatoko, Y. Ishikawa, *Angew. Chem. Int. Ed.* **2001**, *40*, 2323.
[117] H. Maeda, Y. Ishikawa, T. Matsuda, A. Osuka, H. Furuta, *J. Am. Chem. Soc.* **2003**, *125*, 11822.
[118] H. Furuta, T. Ogawa, Y. Uwatoko, K. Araki, *Inorg. Chem.* **1999**, *38*, 2676.
[119] M. Pawlicki, L. Latos-Grażyński, *Chem. Eur. J.* **2003**, *9*, 4650.
[120] J. Hilton, L. H. Sutcliffe, *Prog. NMR Spectrosc.* **1975**, *10*, 27.

Received: January 22, 2007
Published Online: April 24, 2007

